McKean, M. C., Frerman, F. E., & Mielke, D. M. (1979) *J. Biol. Chem. 254*, 2730–2735.
Merrill, A. H., Gidwitz, S., & Bell, R. M. (1982) *J. Lipid Res. 23*, 1368–1372.
Moore, E. G., Cardemil, E., & Massey, V. (1978) *J. Biol. Chem. 253*, 6413–6422.
Moore, E. G., Ghisla, S., & Massey, V. (1979) *J. Biol. Chem. 254*, 8173–8178.
Murfin, W. W. (1974) Ph.D. Thesis, Washington University, St. Louis, MO.
Reinsch, J. W., Feinberg, B. A., & McFarland, J. T. (1980) *Biochem. Biophys. Res. Commun. 94*, 1409–1416.
Rojas, C., Schmidt, J., Lee, M.-Y., Gustafson, W. G., & McFarland, J. T. (1985) *Biochemistry 24*, 2947–2954.
Schulz, H. (1974) *J. Biol. Chem. 249*, 2704–2709.
Stankovich, M. T., & Massey, V. (1976) *Biochim. Biophys. Acta 452*, 335–344.
Steinman, H. M., & Hill, R. L. (1975) *Methods Enzymol. 35*, 136–151.
Stern, J. R. (1961) *Enzymes, 2nd Ed. 5*, 511–529.
Stern, J. R., & del Campillo, A. (1956) *J. Biol. Chem. 218*, 985–1002.
Stern, J. R., del Campillo, A., & Raw, I. (1956) *J. Biol. Chem. 218*, 971–983.
Steyn-Parvé, E. P., & Beinert, H. (1958) *J. Biol. Chem. 233*, 843–852.
Thorpe, C. (1981) *Methods Enzymol. 71*, 366–374.
Thorpe, C., & Massey, V. (1983) *Biochemistry 22*, 2972–2978.
Thorpe, C., Matthews, R. G., & Williams, C. H. (1979) *Biochemistry 18*, 331–337.
Thorpe, C., Ciardelli, T. L., Stewart, C. J., & Wieland, Th. (1981) *Eur. J. Biochem. 118*, 279–282.
Wakil, S. (1956) *Biochim. Biophys. Acta 19*, 497–504.
Wakil, S., & Mahler, H. R. (1954) *J. Biol. Chem. 207*, 125–132.
Wakil, S. J., Green, D. E., Mii, S., & Mahler, H. R. (1954) *J. Biol. Chem. 207*, 631.
Walsh, C., Fisher, J., Spencer, R., Graham, D. W., Ashton, W. T., Brown, J. E., Brown, R. D., & Rogers, E. F. (1978) *Biochemistry 17*, 1942–1951.
Waterson, R. M., & Hill, R. L. (1972) *J. Biol. Chem. 247*, 5258–5265.
Wenz, A., Thorpe, C., & Ghisla, S. (1981) *J. Biol. Chem. 256*, 9809–9812.
Willadsen, P., & Eggerer, H. (1975) *Eur. J. Biochem. 54*, 247–252.

Noncompetitive and Irreversible Inhibition of Xanthine Oxidase by Benzimidazole Analogues Acting at the Functional Flavin Adenine Dinucleotide Cofactor†

Edward B. Skibo
Department of Chemistry, Arizona State University, Tempe, Arizona 85287
Received November 18, 1985; Revised Manuscript Received March 24, 1986

ABSTRACT: Benzimidazole derivatives possessing a leaving group in the 2α-position and either 4,7-dione, 4,7-diol, or 4,7-dimethoxy substituents were examined as inhibitors of buttermilk xanthine oxidase. The quinone and hydroquinone derivatives are not inhibitors of xanthine-oxygen reductase activity, even though the latter is a powerful alkylating agent. The methoxylated hydroquinones are linear noncompetitive inhibitors, the best of which is the 2α-bromo analogue (K_i = 46 μM). During xanthine-oxygen reductase activity, the 2α-bromo analogue irreversibly traps the reduced enzyme. Formation of a C(4a) adduct of the reducted functional FAD cofactor is postulated on the basis of UV–visible spectral evidence and reconstitution of the enzyme after removal of the altered FAD. A probable sequence of events is reversible binding at or near the reduced cofactor followed by adduct formation. It is concluded that potent tight binding inhibitors could be designed that act at the FAD cofactor rather than the purine active site.

It has been shown (Komai & Massey, 1969, 1971) that iodoacetamide inactivates xanthine oxidase in the presence of xanthine by C(4a)-alkylation of the reduced functional FAD cofactor. Described in this paper is a much more potent inhibitor of this type that traps transient reduced enzyme during catalytic cycling, even when present at micromolar concentrations. Also described as a binding site that likely exists near the functional cofactor. Thus far, tight binding inhibitors have been designed that act at or near the hydroxypurine site of the enzyme (Hille & Massey, 1981). This study shows that potent tight binding inhibitors could be designed that act at the FAD cofactor. The implication of this finding is that non-purine-like inhibitors of the enzyme may be designed that could see use as drugs for gout-associated hyperuricemia. Such drugs could have the desirable feature of potent xanthine oxidase inhibition without interference in other aspects of purine metabolism. The current drug of choice allopurinol possesses a purine-like structure and is observed to form nucleotides and nucleosides having antimetabolite potential (McCollister et al., 1964; Chalmers et al., 1969; Krenitsky et al., 1967).

Provided in eq 1 and 2 are the compounds evaluated as inhibitors of the enzyme. 1-Methyl-2-(bromomethyl)benz-

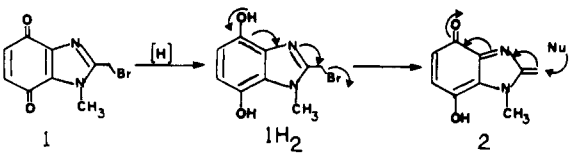

1 $1H_2$ 2 (1)

† This research was supported by a faculty grant-in-aid from Arizona State University, a Cottrell Research Grant from the Research Corp., a grant from the Petroleum Research Foundation, and an award from the National Cancer Institute, DHHS (PHS 1R01CA36876-01).

0006-2960/86/0425-4189$01.50/0

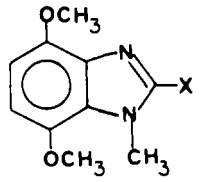

X = CH_2Br, a
= CH_2Cl, b
= CH_2OH, c (2)

3

imidazole-4,7-dione (**1**) represents a potential reductive alkylator (Moore, 1977; Moore & Czerniak, 1981). Thus, reduction to **1**-H_2 will afford the quinone methide species **2**, which has been shown to be an effective nucleophile trap, eq 1 (Skibo, 1986). The methoxylated hydroquinones functionalized with a leaving group at the 2α-position, **3a** and **3b** in eq 2, also represent potential alkylators. It was postulated that the compounds in eq 1 and 2 would interact with the purine binding site of the enzyme since imidazo[4,5-*g*]quinazolines are known to do so (Leonard, 1982). The compounds in eq 1 do not inhibit the enzyme, and the compounds in eq 2 reversibly bind to the enzyme, possibly at or near the functional FAD cofactor. During xanthine-oxygen reductase activity, **3a** eventually alkylates the reduced FAD, resulting in irreversible inhibition.

Materials and Methods

All kinetic measurements were carried out on either a Perkin-Elmer 559 spectrometer or a Perkin-Elmer Lambda-3 spectrometer in which the cell holder had been maintained at 30.0 ± 0.2 °C by circulating thermostated water. The standard deviation of velocities and rate constants ranged from 15 to 20%. Spectra were obtained on a Perkin-Elmer 559 spectrometer and were balanced against 0.05 M pH 7.40 phosphate buffer (μ = 0.1, KCl). Uncorrected melting points were determined with a Mel-Temp apparatus. Elemental analyses were performed by MicAnal Laboratories, Tucson, AZ. TLCs were run with Merck silica gel 60 (F_{254}) plates. IR spectra were taken as thin films on a NaCl plate with a Nicolet MX-1 FTIR spectrophotometer. ^{1}H NMR spectra were taken on a Bruker WH-90 spectrometer. Mass measurements were carried out in the electron-impact mode with a Varian MAT 200 spectrometer. Measurements of pH were made with a Radiometer PHM84 pH meter equipped with a Radiometer GK2401C combination electrode.

Buttermilk xanthine oxidase grade III, FAD, and xanthine were purchased from Sigma Chemical Co. The inorganic salts used in the preparation of buffer solutions were of analytical reagent grade obtained from Mallinkrodt and were used as such. The $CaCl_2 \cdot 2H_2O$ used in cofactor removal was recrystallized (ethanol) analytical reagent-grade material. The buffer solutions were prepared in doubly glass-distilled water.

The preparation of **1**-H_2, **3b**, and **3c** was carried out as previously described (Skibo, 1986). The preparation of **1** and **3a** was carried out as described below.

1-Methyl-2-(bromomethyl)benzimidazole-4,7-dione (**1**). A mixture consisting of 660 mg (1.95 mmol) of the hydrobromide salt of **1**-H_2 and 2.10 g (7.8 mmol) of $FeCl_3 \cdot 6H_2O$ in 10 mL of water was stirred for 5 min. The partially precipitated product was removed by extraction with 3 × 15-mL portions of chloroform. The extracts were dried over $MgSO_4$, filtered, and concentrated to ~5 mL. Addition of hexane afforded analytically pure **1** as yellow flakes: yield 407 mg (82%); mp 148–149 °C dec; TLC (10% ethanol in chloroform) on silica gel, R_f 0.54; IR (thin film) 1662, 1590, 1527, 1507, 1478, 1277, 1220, and 1053 cm^{-1}; ^{1}H NMR ($CDCl_3$) δ 6.69 and 6.68 (2 H, d, 5-H and 6-H), 4.58 (2 H, s, $-CH_2Br$), and 4.04 [3 H, s, N(1)–CH_3]; mass spectrum (EI mode), *m/e* 254 (M^+), 256 ($M^+ + 2$), 175 ($M^+ - {}^{79}Br$). Anal. Calcd for $C_9H_7BrN_2O_2$: C, 42.36; H, 2.76; N, 10.97. Found: C, 42.39; H, 2.66; N, 10.89.

1-Methyl-2-(bromomethyl)-4,7-dimethoxybenzimidazole (**3a**). A mixture of 0.40 g (1.80 mmol) of **3c** and 0.5 mL (5.6 mmol) of PBr_3 in 25 mL of chloroform was heated at reflux for 1 h. The reaction mixture was then chilled and diluted to 100 mL with diethyl ether. Precipitate solids were removed by filtration and dissolved in 50 mL of water. The aqueous solution was filtered and then buffered to pH 6 with bicarbonate, resulting in crystallization of **3a**. The crystals were removed by filtration after being chilled for 12 h and recrystallized from hexane/chloroform: yield 0.38 g (75%); mp 245–50 °C dec; TLC (10% ethanol in chloroform) on silica gel, R_f 0.82; IR (thin film) 2951, 2933, 1523, 1464, 1262, and 1098 cm^{-1}; ^{1}H NMR ($CDCl_3$) δ 6.47 and 6.63 (2 H, AB system, J = 9 Hz, aromatic protons), 4.58 (2 H, s, $-CH_2Br$) 4.08 (3 H, s, N(3)–CH_3), and 3.90 and 3.96 (6 H, 2 s, 4,7-dimethoxy). Anal. Calcd for $C_{11}H_{13}BrN_2O_2$: C, 46.32; H, 4.59; N, 9.81. Found: C, 46.03; H, 4.53; N, 9.67. pK_a for acid dissociation of the N(3)-protonated form is 4.09 ± 0.06. UV–visible spectra [λ_{max} (nm) ϵ] showed the following: **3a**, 236, 3.06 × 10^4; 275, 1.28 × 10^4. **3a**·H$^+$, 240, 4 × 10^4; 278, 7400; [308], 4600.

Hydrolysis Products of **3a**. (*A*) *First-Phase Product.* Dissolution of 25 mg (0.087 mmol) of **3a** in 10 mL of methanol was followed by dilution to 100 mL with 0.2 M pH 8.00 phosphate buffer (μ = 1.0, KCl). The reaction was incubated at 30 °C for 1 h (representing 2.7 half-lives of the first phase). The first-phase product was removed by extraction with 7 × 5-mL portions of chloroform. Drying of the chloroform extracts ($MgSO_4$) was followed by filtration and concentration to an oil. ^{1}H NMR, IR (thin film), and TLC (10% ethanol in chloroform on silica gel) results were consistent with those of **3b** (Skibo, 1986). The 16.3 mg obtained represents a crude yield of 77%. The TLC above did indicate the presence of trace amounts of the alcohol with R_f 0.76.

(*B*) *Second-Phase Products.* A reaction mixture consisting of 22.8 mg (0.08 mmol) of **3a** in 10 mL of methanol and 90 mL of 0.2 M pH 7.00 phosphate buffer (μ = 1.0, KCl) was incubated for 4 days at 30 °C. The reaction mixture was then extracted 10 times with 10-mL portions of chloroform. Drying of the extracts over $MgSO_4$ followed by filtration and concentration afforded 11.5 mg (64%) of pure **3c**. Identity is based on IR and TLC comparison with authentic material (Skibo, 1986).

Azide Trapping Study with **3a** *at pH 7.00.* Dissolution of 25 mg (0.087 mmol) of **3a** in 10 mL of methanol was followed by dilution to 100 mL with 0.2 M pH 7.00 phosphate buffer (μ = 1.0, KCl) containing 55 mg (0.84 mmol) of sodium azide. Incubation at 30 °C was carried out for 2 days. The reaction was then extracted 5 times with 10 mL of chloroform. Organic extracts were washed 2 times with 25-mL volumes of H_2O and then dried ($MgSO_4$). Concentration in vacuo afforded 19.7 mg (90%) of an oil identified as the 2α-azido derivative. A repeat of this experiment afforded a yield of 70%. TLC (5% ethanol in chloroform on silica gel) gave R_f 0.9. ^{1}H NMR ($CDCl_3$) gave δ 5.58 and 6.51 (2 H, AB quartet, J = 8.6 Hz, aromatic), 4.59 (2 H, s, azidomethyl), 4.05 (3 H, s, N(1)–methyl), and 3.96 and 3.89 (6 H, 2 s, 4,7-dimethoxy). IR (thin film) gave 2921, 2850, 2097 (N_3), 1521, 1492, and 1260 cm^{-1}.

Xanthine Oxidase Inhibition Studies. Inhibition of xanthine-oxygen reductase activity was studied in 0.05 M pH 7.40 phosphate buffer (μ = 0.1, KCl) containing 22 μM ethylenediaminetetraacetic acid (EDTA) at 30 °C. Unless oth-

erwise state, the concentration of enzyme employed was 0.034 μM (per enzyme-bound FAD), and xanthine concentrations ranged from 2 to 20 μM. The molarity of enzyme was determined from an absorbance measurement at 450 nm and the ϵ_{450} value of 37 800 M^{-1} cm^{-1} per enzyme-bound FAD (Massey et al., 1969). The xanthine oxidase employed, grade III (Sigma), is chromatographically pure and reported to contain 10 units/mL. Stock solutions of the hydrobromide salts of **3** and **1**-H_2, as well as **1**, were prepared with dimethyl sulfoxide. In the case of **3a**, the stock solution was prepared fresh each day since slow solvolysis results in a loss of activity. The xanthine-oxygen reductase activity was monitored by following uric acid formation at 290 nm. The measurement of maximum velocities, V_{max} (μM s^{-1}), was carried out in the presence of 72 μM xanthine. These velocities reasonably approximate extrapolated values but higher xanthine concentrations resulted in decreases in velocity. Concentrated stock solutions of inactivated enzyme for spectral studies were prepared by reacting 3.2 μM xanthine oxidase with 1.78×10^{-4} M xanthine and 7×10^{-4} M **3a** in aerobic buffer for 5 min. Spectral studies were carried out immediately after preparation of the inactivated enzyme solution.

Large-Scale Preparation of Inhibited Xanthine Oxidase and FAD Cofactor Removal. Combination of a dimethyl sulfoxide solution of **3a**·HBr with an aerobic solution of native enzyme in 0.05 M pH 7.40 phosphate buffer (μ = 0.1, KCl) was followed by addition of a xanthine solution in the same buffer. The reaction mixture was then stirred for 2 min at room temperature. The volume of the reaction mixture was 20 mL and initially contained the following concentrations of reactants: **3a**, 727 μM; enzyme, 4.8 μM; xanthine, 111 μM. The concentration of dimethyl sulfoxide by volume in the reaction mixture was 2%. The treated enzyme possessed no detectable xanthine-oxygen reductase activity. Denaturation of the protein was observed when inhibited enzyme was prepared at lower dilutions than employed above and when high dilution reactions were allowed to sit at room temperature for long periods of time (>1 h).

Chilling the reaction mixture in an ice bath was followed by addition of 8 g (0.4 g/mL of reaction volume) of ammonium sulfate. After additional chilling for 20 min, the mixture was centrifuged for 30 min at 12000*g* in a Servall preparative centrifuge. The protein pellet was dissolved in a minimum amount (~1.0 mL) of 0.1 M tris(hydroxymethyl)aminomethane (Tris) pH 8.00 buffer containing 1 mM salicylate, 0.3 mM EDTA, and 10 mM cysteine and then dialyzed for 24 h against the same buffer. During this period, four changes of the dialyzing fluid were made. Removal of the FAD cofactor by $CaCl_2$ treatment, as described by Komai et al. (1969), resulted in extensive denaturation of the enzyme. This is probably due to the lower concentrations of enzyme employed in this study; <10 mg/mL vs. ~40 mg/mL in the procedure described by the above workers. To minimize denaturation, glycerin (10% of the volume) was added to the dialyzed solution of inactivated enzyme. Chilling this mixture to 5 °C was followed by addition of solid $CaCl_2 \cdot 2H_2O$ (170 mg/mL). The resulting mixture was then stirred at 20 °C for 90 min. The isolation of the deflavoenzyme and its reconstitution with FAD were carried out as described by Komai et al. (1969).

Results and Discussion

Chemistry of Title Systems. To assess the reactivity of the title systems, hydrolysis and nucleophilic substitution reactions were studied in aqueous buffer (μ = 1.0, KCl, at 30 °C). The fate of **1**-H_2 in anaerobic aqueous buffer has been described (Skibo, 1986). Elimination of bromide to afford **2** occurs at 0.22 s^{-1} from the 4-hydroxy anion of **1**-H_2 (pK_a = 8.13). At pH 7.40, only a fraction of **1**-H_2 is ionized, and the observed first-order rate constant for elimination is 0.034 s^{-1}. Nucleophilic trapping of **2** occurs by a non-rate-determining Michael addition that is irreversible if a strong nucleophile is involved. In contrast to the reactivity of **1**-H_2, **1** is stable in 0.05 M pH 7.40 phosphate buffer. Thus, **1** will become an alkylator only when reduced to the hydroquinone form (hence the term reductive alkylator).

The hydrolysis of **3a** (5×10^{-5} M) was studied in aerobic 0.2 M phosphate buffer over the pH range of 6.0–8.0. The course of hydrolysis was followed spectrophotometrically at 240 nm. Absorbance (240 nm) vs. time (s) plots evidenced a two consecutive first-order rate law (Alcock et al., 1970). The observed rate constants for the first and second kinetic phase, $k_{obsd} = 5.2 \times 10^{-4}$ s^{-1} and $k'_{obsd} = 1.23 \times 10^{-5}$ s^{-1}, respectively, are independent of pH and 10-fold changes in buffer. Product studies (see Materials and Methods) indicate that 1-methyl-2-(chloromethyl)-4,7-dimethoxybenzimidazole (**3b**) and a trace amount of the 2-hydroxymethyl derivative (**3c**) are the hydrolysis intermediates and that **3c** is the only final product. Consistent with **3b** as the intermediate responsible for the second kinetic phase, authentic **3b** hydrolyzes to **3c** at $k_{obsd} = 1 \times 10^{-5}$ s^{-1}. The pK_a values for acid dissociation from the N(3)-protonated forms of **3a** and **3b** are 4.09 and 4.10, respectively (Skibo, 1986). Thus, the reactants are predominately in the neutral form over the pH range studied. The pH independence of k_{obsd} and k'_{obsd} indicates that protons and hydroxide are not involved in any rate-determining step. The sequence of hydrolysis, **3a** → **3b** + **3c** and then **3b** → **3c**, is best explained by the mechanism found in eq 3. According

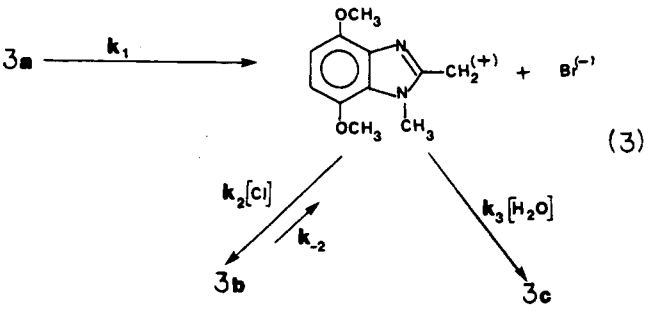

(3)

to this mechanism, the first kinetic phase pertains to rate-determining carbocation formation from **3a** at k_1 (s^{-1}). Thus, the experimental value of k_{obsd} is considered to be equal to k_1. The first-phase products, **3b** and **3c**, arise as a result of carbocation trapping by chloride and water, respectively. The **3b** thus formed in this reaction re-forms the carbocation species by a reversible process resulting in the second kinetic phase. Irreversible trapping of the carbocation by water affords the second kinetic phase product **3c**. Consideration of steady-state carbocation concentrations during the conversion of **3b** to **3c** indicates that k'_{obsd} is equal to $k_3k_{-2}/(k_2[Cl] + k_3)$. To test for a carbocation mechanism, azide was added to reaction mixtures at concentrations 10–200 times that of **3a**. The rates of hydrolysis were seen to be independent of [azide], but the 2-azidomethyl derivative was obtained from the completed reaction (see Materials and Methods). These findings are consistent with rate-determining formation of a carbocation, which is selectively trapped by azide (Ingold, 1969).

The results of hydrolysis studies presented above indicate that **1**-H_2, **3a**, and **3b** are sufficiently long lived in aqueous buffer to bind and perhaps alkylate the enzyme. Eventual hydrolysis does preclude long incubation experiments, however.

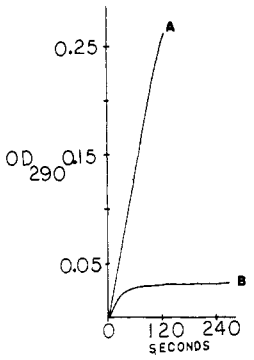

FIGURE 1: (A) Plot of OD (290 nm) vs. time (s) for the oxidation of 36 μM xanthine by 0.034 μM xanthine oxidase in aerobic 0.05 M pH 7.40 phosphate buffer. (B) Plot of OD (290 nm) vs. time for the same reaction in the presence of 33 μM inhibitor. Absorbance at t = 0 is set at zero.

Enzyme Binding Studies. Compounds **1**, **1**-H_2, **3a**, **3b**, and **3c** were examined as inhibitors of xanthine oxidation by 0.034 μM xanthine oxidase in 0.05 M pH 7.40 phosphate buffer (μ = 0.1, KCl) at 30 °C. Incubation of xanthine-reduced and oxidized xanthine oxidase with **1**-H_2 (up to 42 μM) under strictly anaerobic conditions for 5 min did not result in inhibition. Studies with **1** (up to 265 μM) over much longer incubation times provided the same result. All the compounds in eq 2 were linear noncompetitive inhibitors but **3a** inactivated the enzyme during catalytic cycles.

When uric acid formation was monitored in an aerobic 3-mL reaction containing **3a** (33 μM) and xanthine (36 μM), a burst at 290 nm was noted followed by termination far below the expected final absorbance of uric acid, Figure 1. Addition of 1 mL of 216 μM xanthine after termination (immediately or after 1 h) did not result in uric acid formation, suggesting that inhibition is irreversible. Incubation of oxidized enzyme with **3a** for up to 10 min prior to xanthine addition had no effect on the burst and subsequent termination. On the other hand, incubation of xanthine-reduced enzyme (0.034 μM) with **3a** (6.7 μM) for 2 min resulted in complete inactivation. Thus, **3a** is likely trapping reduced enzyme during xanthine-oxygen reductase activity. Provided in Figure 2 are UV–visible spectra of 3.2 μM oxidized native enzyme and 3.2 μM inactivated enzyme prepared under aerobic conditions (see Materials and Methods). The difference spectrum (native oxidized vs. inactive enzyme) found in the inset of Figure 2 shows an absorbance maximum at 450 nm with a shoulder at 480 nm, both of which are associated with the oxidized FAD cofactor (Komai et al., 1969). The $\Delta\epsilon$ value at 450 nm accompanying inactivation is ~9000 M^{-1} cm^{-1}, on the basis of 3.2 μM of enzyme-bound FAD, a value somewhat less than the ~12000 M^{-1} cm^{-1} expected for loss of one enzyme-bound FAD (Komai et al., 1969). It is postulated that one enzyme-bound FAD is actually lost upon **3a** inactivation. The inhibitor possesses an intense absorbance maximum at 275 nm, which trails into the visible region and could thereby lower the $\Delta\epsilon$ value at 450 nm. Consistent with the loss of only the FAD cofactor, the inactivated enzyme spectrum resembles that of deflavoenzyme (Komai et al., 1969). Inspection of Figure 2 reveals that the native and inactivated enzyme spectra are nearly identical above 530 nm and that the latter spectrum possesses abosrbance maxima at 420 and 467 nm (shown with arrows) associated with the Fe–S centers. The same results were obtained when anaerobic xanthine-reduced enzyme was treated with **3a**. Although an FAD is apparently lost upon inactivation, incubation of inactivated enzyme (0.085 μM) with FAD (32 μM) did not restore activity.

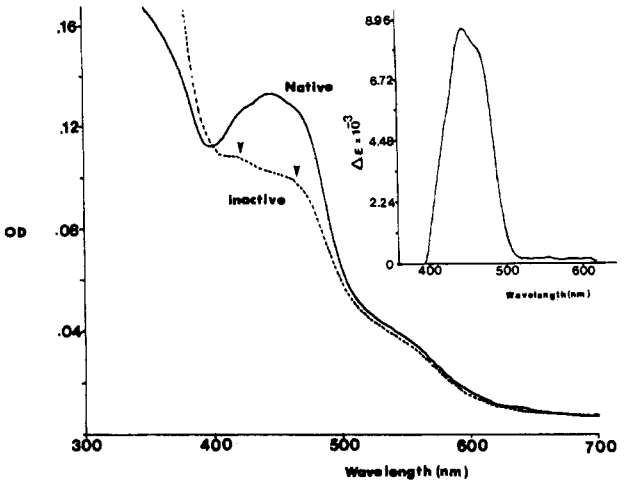

FIGURE 2: (—) Spectrum of 3.2 μM xanthine oxidase in aerobic 0.05 M pH 7.40 phosphate buffer. (--) Spectrum of 3.2 μM xanthine oxidase in aerobic 0.05 M pH 7.40 phosphate buffer after treatment with 1.78×10^{-4} M xanthine and 1.4×10^{-3} M **3a**. Found in the inset is a plot of $\Delta\epsilon$, based on 3.2 μM enzyme-bound FAD, vs. wavelength (nm).

The findings enumerated above suggest that **3a** inactivates the enzyme by forming an adduct with the reduced FAD involved in xanthine-oxygen reductase activity. The adduct is apparently both bound to the enzyme and stable to oxygen, resulting in the loss of the oxidized FAD spectrum. If aerobic inactivation pertains to cofactor alteration, then removal of the altered cofactor by $CaCl_2$ treatment (Komai et al., 1969) followed by incubation with FAD will afford native enzyme. Bulk **3a**-inactivated enzyme, possessing no detectable xanthine-oxygen reductase activity, was treated with $CaCl_2$ according to the modified procedure found under Material and Methods. Xanthine-oxygen reductase activity was restored upon treating the deflavoenzyme thus obtained with FAD.

The above findings bear a close resemblance to those of Bray and Watts (1966), Bray et al. (1966), McGartoll and Bray (1969), and Komai and Massey (1969, 1971) regarding iodoacetamide inactivation of the enzyme. The latter workers showed that formation of a C(4a) adduct of the reduced

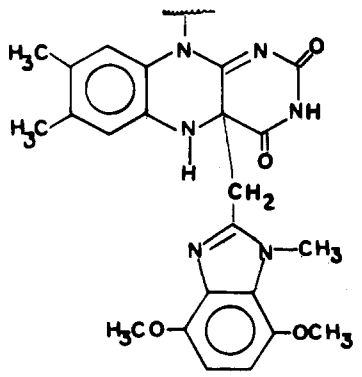

C(4a)-Adduct

functional FAD is the primary process in inactivation. Likewise, formation of the C(4a) adduct is postulated to be involved in **3a** inactivation of the enzyme.

The following observations suggests that this adduct is formed: (i) the adduct is oxygen stable; (ii) the adduct does not contribute to the visible spectrum above 400 nm resulting in the apparent loss of 1 FAD; (iii) the adduct could be photoeliminated. It has been shown that C(4a) adducts of reduced flavin are oxygen-stable (Ghisla et al., 1973). An

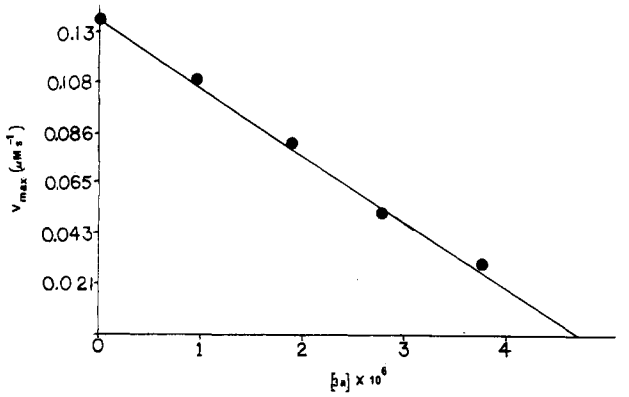

FIGURE 3: Plot of V_{max} (μM s^{-1}) for xanthine oxidation vs. [**3a**]. Aerobic 2-mL reaction mixtures consisting of 0.050 μM enzyme, 26 μM xanthine, and various concentrations of **3a** were incubated at 30 °C until termination. The V_{max} (μM s^{-1}) values were then measured after addition of 1 mL of 2.16×10^{-4} M xanthine. Provided on the plot are the [**3a**] values after dilution with xanthine stock.

N(5) adduct, on the other hand, would be readily oxidized by oxygen (Hemmerich et al., 1981; Bruice & Eberline, 1982). It has also been shown that the C(4a) adducts of reduced flavins do not absorb strongly above 400 nm (Komai & Massey, 1969, 1971; Ghisla et al., 1973). Komai & Massey (1971) have shown that the C(4a) adduct obtained upon iodoacetamide inactivation could be photoeliminated. Irradiation of 3.2 μM **3a**-inactivated enzyme in aerobic 0.05 M pH 7.40 phosphate buffer was carried out for 10 min, employing a 450-W medium pressure mercury lamp, equipped with a Pyrex filter, from a distance of 6 in. The UV–visible spectrum obtained after irradiation indicated a partial return of the FAD absorbance maximum at 450 nm. Accompanying the spectral change was a partial return of xanthine-oxygen reductase activity.

To assess the minimum concentration of inhibitor needed to inactivate the enzyme, titration was carried out with limited amounts of inhibitor. The maximum velocities in μM s^{-1} (V_{max}) were measured after termination of aerobic reaction mixtures consisting of 0.050 μM enzyme, 26 μM xanthine, and various concentrations of inhibitor. Found in Figure 3 is the plot of V_{max} vs. [**3a**] thus obtained. Extrapolation to V_{max} = 0 indicates that complete inactivation occurs under these conditions when [**3a**]/[XO] = 138. The excess inhibitor required may pertain to equilibrium binding occurring prior to alkylation as well as hydrolysis of **3a** to the inactive species **3b** and **3c** (vide infra).

It was noted that the initial burst of uric acid formation in the presence of **3a** (plot B in Figure 1) was associated with a velocity somewhat less than the burst in the absence of inhibitor (plot A in Figure 1). To assess whether the decrease in velocity resulted from reversible or irreversible loss of enzyme activity during the burst, V_{max} vs. [XO] was plotted for the initial burst in the presence and absence of inhibitor (plots not shown). Both plots possess a zero intercept, but the inhibitor plot possesses a lower slope than the plot without inhibitor. Thus, **3a** is reversibly binding to the enzyme in a noncompetitive fashion during the initial burst. Irreversible inactivation, on the other hand, would have resulted in an intercept at a positive value of [XO] (Segal, 1975). The Lineweaver-Burk plot found in Figure 4 reveals that **3a** is a linear noncompetitive inhibitor with K_i = 34 μM. Compounds **3b** and **3c** are also linear noncompetitive inhibitors with K_i values of 310 μM and ~1500 μM, respectively (Lineweaver-Burk plots not shown). Compounds **3b** and **3c** did not alkylate the enzyme during catalytic cycles, however.

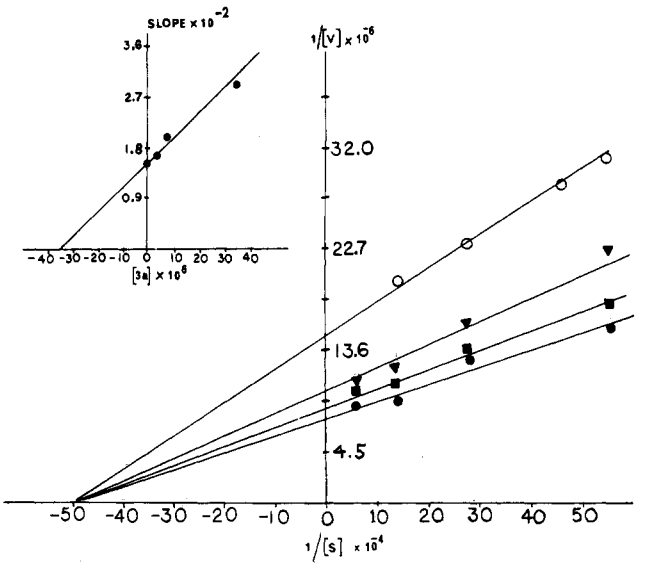

FIGURE 4: Lineweaver-Burk plot employing [XO] = 0.034 μM and xanthine as substrate (S) in pH 7.40 phosphate buffer at 30 °C. The concentrations of **3a** are: (●) 0, (■) 3.36, (▼) 6.73, and (○) 34.6 μM. The Dixon plot found in the inset indicates that K_i = 34 μM.

Since **3a** eventually alkylates the functional FAD cofactor, it is reasonable to assume that **3a**, as well as the other methoxylated hydroquinones, binds at or near this cofactor. Linear noncompetitive inhibition suggests that inhibitor and substrate are binding independently and that the inhibitor–substrate–enzyme complex is inactive, perhaps because of the absence of electron transfer to or from the cofactor. Considering the mechanism of **3a** hydrolysis, alkylation of the reduced cofactor by bound **3a** could occur via a carbocation intermediate. These views explain the excess of **3a** required for complete inactivation and the lack of alkylation by **1**-H_2 and **3b**, even though these compounds possess a leaving group. During catalytic cycling, **3a** must be present in excess so as to compete with oxygen for binding at the reduced cofactor. Even under anaerobic conditions, excess amounts of **3a** are required so that binding and inactivation of the enzyme could occur before hydrolysis. In contrast, **3b** binds poorly, and **1**-H_2 does not bind at all; thus, these compounds do not alkylate the cofactor. The binding site appears to be quite sensitive to the structure of the inhibitor; the quinone (**1**) and hydroquinone (**1**-H_2) derivatives do not bind, and changes in the 2α-substituent of the methoxylated hydroquinone (notably **3c**) severely decrease binding. Currently, efforts are under way to define the binding site further and design more potent inhibitors.

CONCLUSIONS

It is concluded that the methoxylated hydroquinones in eq 2 bind at or near the functional FAD cofactor of xanthine oxidase and that **3a** traps the reduced cofactor by C(4a) adduct formation. The **3a** inactivation of the enzyme is much like iodoacetamide inactivation except that anaerobic conditions and high inhibitor concentrations are not required. Thus, **3a** represents a potent non-purine-like inhibitor of xanthine oxidase, which may act without interfering with other aspects of purine metabolism.

ACKNOWLEDGMENTS

I thank D. E. Lohr of Arizona State University for helpful discussions concerning FAD cofactor removal.

Registry No. **1**, 99922-35-7; **1**-H_2, 99922-37-9; **1**-H_2 (HBr salt), 99922-30-2; **3a**, 103003-03-8; **3b**, 99922-29-9; **3c**, 99922-28-8; FAD, 146-14-5; xanthine oxidase, 9002-17-9.

REFERENCES
Alcock, N. W., Benton, D. J., & Moore, P. (1970) *Trans. Faraday Soc. 66*, 2210–2213.
Bray, R. C., & Watts, D. C. (1966) *Biochem. J. 98*, 142–148.
Bray, R. C., Chisholm, A. J., Hart, L. I., Meriwether, L. S., & Watts, D. C. (1966) in *Flavins and Flavoproteins* (Slater, E. C., Ed.) p 117, Elsevier, Amsterdam.
Chalmers, R. E., Parker, R., Simmonds, H. A., Snedden, W., & Watts, R. W. E. (1969) *Biochem. J. 112*, 527–532.
Eberlein, G., & Bruice, T. C. (1982) *J. Am. Chem. Soc. 104*, 1449–1452.
Ghisla, S., Hartmann, U., Hemmerich, P., & Müller, F. (1973) *Justus Liebigs Ann. Chem.*, 1388–1414.
Hemmerich, P., Massey, V., Michel, H., & Schug, C. (1981) *Struct. Bonding (Berlin) 48*, 93–121.
Hille, R., & Massey, V. (1981) *Pharmac. Ther. 14*, 249–263.
Ingold, C. K. (1969) *Structure and Mechanism in Organic Chemistry*, pp 467–468, Cornell University Press, Ithaca, New York.
Komai, H., & Massey, V. (1969) *Fed. Proc., Fed. Am. Soc. Exp. Biol. 28*, 868.
Komai, H., & Massey, V. (1971) in *Proceedings of the Third International Symposium on Flavins and Flavoproteins* (Kamin, H., Ed.) pp 399–423, University Park Press, Baltimore, MD.
Komai, H., Massey, V., & Palmer, G. (1969) *J. Biol. Chem. 244*, 1692–1700.
Krenitsky, T. A., Elion, G. B., Strelitz, R. A., & Hitchings, G. H. (1967) *J. Biol. Chem. 242*, 2675–2682.
Leonard, N. J. (1982) *Acc. Chem. Res. 15*, 128–135.
Massey, V., Brumby, P. E., Komai, H., & Palmer, G. (1969) *J. Biol. Chem. 244*, 1682–1691.
McCollister, R. J., Gilbert, W. R., Jr., Ashton, D. M., & Wyngaarden, J. B. (1964) *J. Biol. Chem. 239*, 1560–1568.
McGartoll, M. A., & Bray, R. C. (1969) *Biochem. J. 114*, 443–444.
Moore, H. W. (1977) *Science (Washington, D.C.) 197*, 527–532.
Moore, H. W., & Czerniak, P. (1981) *Med. Res. Rev. 1*, 249–280.
Segel, I. H. (1975) *Enzyme Kinetics*, p 128, Wiley, New York.
Skibo, E. B. (1986) *J. Org. Chem. 51*, 522–527.

Crystal Structure of a Novel Trimethoprim-Resistant Dihydrofolate Reductase Specified in *Escherichia coli* by R-Plasmid R67†

David A. Matthews,*,‡ S. L. Smith,§ D. P. Baccanari,§ J. J. Burchall,§ S. J. Oatley,‡ and J. Kraut‡

Department of Chemistry, University of California—San Diego, La Jolla, California 92093, and Burroughs Wellcome Company, Research Triangle Park, North Carolina 27709

Received January 3, 1986; Revised Manuscript Received March 21, 1986

ABSTRACT: Crystalline R67 dihydrofolate reductase (DHFR) is a dimeric molecule with two identical 78 amino acid subunits, each folded into a β-barrel conformation. The outer surfaces of the three longest β strands in each protomer together form a third β barrel having six strands at the subunit interface. A unique feature of the enzyme structure is that while the intersubunit β barrel is quite regular over most of its surface, an 8-Å "gap" runs the full length of the barrel, disrupting potential hydrogen bonds between β-strand D in subunit I and the adjacent corresponding strand of subunit II. It is proposed that this deep groove is the NADPH binding site and that the association between protein and cofactor is modulated by hydrogen-bonding interactions along one face of this antiparallel β-barrel structure. A hypothetical model is proposed for the R67 DHFR–NADPH–folate ternary complex that is consistent with both the known reaction stereoselectivity and the weak binding of 2,4-diamino inhibitors to the plasmid-specified reductase. Geometrical comparison of this model with an experimentally determined structure for chicken DHFR suggests that chromosomal and type II R-plasmid specified enzymes may have independently evolved similar catalytic machinery for substrate reduction.

Dihydrofolate reductase (DHFR; EC 1.5.1.3)[1] is a very widely occurring enzyme that catalyzes the NADPH-dependent reduction of 7,8-dihydrofolate to 5,6,7,8-tetrahydrofolate. Trimethoprim (TMP) selectively inhibits bacterial DHFR and for the past 15 years has been used clinically in combination with sulfonamides as a broad spectrum antibiotic. In 1972 Fleming et al. reported that certain clinical strains of *Escherichia coli* and *Klebsiella aerogenes* carry R factors that confer high levels of resistance to TMP. In accord with already known mechanisms by which R factors confer resistance to other drugs, it was anticipated that in this case as well resistance would most likely occur because of drug inactivation or impermeability (Amyes & Smith, 1974; Benveniste & Davies, 1973). However, it was subsequently shown by Amyes and Smith (1974) and Skold and Widh (1974) that plasmids in these resistant organisms coded for a novel DHFR

† Supported by U.S. Public Health Service, National Institutes of Health, Research Grant CA17374.

* Address correspondence to this author at the Agouron Institute, 505 Coast Boulevard South, La Jolla, CA 92037.
‡ University of California—San Diego.
§ Burroughs Wellcome Co.

[1] Abbreviations: DHFR, dihydrofolate reductase; NADPH, nicotinamide adenine dinucleotide phosphate; MTX, methotrexate; DTT, dithiothreitol; MPD, 2-methyl-2,4-pentanediol; NMN, nicotinamide mononucleotide; AMN, adenosine 2′,5′-phosphate; TMP, trimethoprim.

0006-2960/86/0425-4194$01.50/0